

NUSTAR AND XMM-NEWTON OBSERVATIONS OF LUMINOUS, HEAVILY OBSCURED, WISE-SELECTED QUASARS AT $Z \sim 2$

D. STERN¹, G. B. LANSBURY², R. J. ASSEF³, W. N. BRANDT^{4,5}, D. M. ALEXANDER², D. R. BALLANTYNE⁶, M. BALOKOVIĆ⁷,
D. BENFORD⁸, A. BLAIN⁹, S. E. BOGGS¹⁰, C. BRIDGE⁷, M. BRIGHTMAN¹¹, F. E. CHRISTENSEN¹², A. COMASTRI¹³, W. W. CRAIG^{10,14},
A. DEL MORO², P. R. M. EISENHARDT¹, P. GANDHI², R. GRIFFITH⁴, C. J. HAILEY¹⁵, F. A. HARRISON⁷, R. C. HICKOX¹⁶,
T. H. JARRETT¹⁷, M. KOSS¹⁸, S. LAKE¹⁹, S. M. LAMASSA²⁰, B. LUO^{4,5}, C.-W. TSAI¹, D. J. WALTON⁷, E. L. WRIGHT¹⁹, J. WU¹⁹,
L. YAN²¹ AND W. W. ZHANG⁸

Draft 3.0 — March 10, 2014

ABSTRACT

We report on a *NuSTAR* and *XMM-Newton* program that has observed a sample of three extremely luminous, heavily obscured *WISE*-selected AGN at $z \sim 2$ in a broad X-ray band (0.1 – 79 keV). The parent sample, selected to be faint or undetected in the *WISE* 3.4 μ m (*W1*) and 4.6 μ m (*W2*) bands but bright at 12 μ m (*W3*) and 22 μ m (*W4*), are extremely rare, with only ~ 1000 so-called “*W1W2*-dropouts” across the extragalactic sky. Optical spectroscopy reveals typical redshifts of $z \sim 2$ for this population, implying rest-frame mid-IR luminosities of $\nu L_\nu(6\mu\text{m}) \sim 6 \times 10^{46} \text{ erg s}^{-1}$ and bolometric luminosities that can exceed $L_{\text{bol}} \sim 10^{14} L_\odot$. The corresponding intrinsic, unobscured hard X-ray luminosities are $L(2 - 10 \text{ keV}) \sim 4 \times 10^{45} \text{ erg s}^{-1}$ for typical quasar templates. These are amongst the most luminous AGN known, though the optical spectra rarely show evidence of a broad-line region and the selection criteria imply heavy obscuration even at rest-frame 1.5 μ m. We designed our X-ray observations to obtain robust detections for gas column densities $N_{\text{H}} \leq 10^{24} \text{ cm}^{-2}$. In fact, the sources prove to be fainter than these predictions. Two of the sources were observed by both *NuSTAR* and *XMM-Newton*, with neither being detected by *NuSTAR* ($f_{3-24 \text{ keV}} \lesssim 10^{-13} \text{ erg cm}^{-2} \text{ s}^{-1}$), and one being faintly detected by *XMM-Newton* ($f_{0.5-10 \text{ keV}} \sim 5 \times 10^{-15} \text{ erg cm}^{-2} \text{ s}^{-1}$). A third source was observed only with *XMM-Newton*, yielding a faint detection ($f_{0.5-10 \text{ keV}} \sim 7 \times 10^{-15} \text{ erg cm}^{-2} \text{ s}^{-1}$). The X-ray data require gas column densities $N_{\text{H}} \gtrsim 10^{24} \text{ cm}^{-2}$, implying the sources are extremely obscured, consistent with Compton-thick, luminous quasars. The discovery of a significant population of heavily obscured, extremely luminous AGN does not conform to the standard paradigm of a receding torus, in which more luminous quasars are less likely to be obscured. If a larger sample conforms with this finding, then this suggests an additional source of obscuration for these extreme sources.

Subject headings: infrared: AGN — galaxies: active — AGN: individual (WISEA J181417.29+341224.8, WISEA J220743.82+193940.1, WISEA J235710.82+032802.8)

¹ Jet Propulsion Laboratory, California Institute of Technology, 4800 Oak Grove Drive, Mail Stop 169-221, Pasadena, CA 91109, USA [e-mail: daniel.k.stern@jpl.nasa.gov]

² Department of Physics, University of Durham, South Road, Durham DH1 3LE, UK

³ Núcleo de Astronomía de la Facultad de Ingeniería, Universidad Diego Portales, Av. Ejército Libertador 441, Santiago, Chile

⁴ Department of Astronomy and Astrophysics, The Pennsylvania State University, 525 Davey Lab, University Park, PA 16802, USA

⁵ Institute for Gravitation and the Cosmos, The Pennsylvania State University, University Park, PA 16802, USA

⁶ Center for Relativistic Astrophysics, School of Physics, Georgia Institute of Technology, Atlanta, GA 30332, USA

⁷ Cahill Center for Astronomy and Astrophysics, California Institute of Technology, Pasadena, CA 91125, USA

⁸ NASA Goddard Space Flight Center, Greenbelt, MD 20771, USA

⁹ Physics & Astronomy, University of Leicester, 1 University Road, Leicester, LE1 7RH, UK

¹⁰ Space Sciences Laboratory, University of California, Berkeley, 7 Gauss Way, Berkeley, CA 94720-7450, USA

¹¹ Max-Planck-Institut für extraterrestrische Physik, Giessenbachstrasse 1, D-85748, Garching bei München, Germany

¹² Danish Technical University, DK-2800 Lyngby, Denmark

¹³ INAF Osservatorio Astronomico di Bologna, via Ranzani 1, I-40127, Bologna, Italy

¹⁴ Lawrence Livermore National Laboratory, Livermore, CA 94550, USA

¹⁵ Columbia Astrophysics Laboratory, Columbia University, New York, NY 10027, USA

¹⁶ Department of Physics and Astronomy, Dartmouth College, 6127 Wilder Laboratory, Hanover, NH 03755, USA

¹⁷ Astrophysics, Cosmology and Gravity Centre, Department of Astronomy, University of Cape Town, Rondebosch, South Africa

¹⁸ Institute for Astronomy, Department of Physics, ETH Zurich, Wolfgang-Pauli-Strasse 27, CH-8093 Zurich, Switzerland

¹⁹ Division of Astronomy & Astrophysics, University of California, Los Angeles, Los Angeles, CA 90095-1547, USA

²⁰ Department of Physics and Yale Center for Astronomy and Astrophysics, Yale University, New Haven, CT 06520-8120, USA

²¹ Infrared Processing and Analysis Center, Department of Astronomy, California Institute of Technology, Pasadena, CA 91125, USA

1. INTRODUCTION

The *Wide-field Infrared Survey Explorer* (*WISE*) (Wright et al. 2010) is an extremely capable and efficient black hole finder. As demonstrated in selected fields by *Spitzer* (e.g., Stern et al. 2005; Donley et al. 2012), the same material that obscures AGN at UV, optical and soft X-ray energies is heated by the AGN and emits strongly at mid-IR wavelengths. The all-sky *WISE* survey identifies millions of obscured and unobscured quasars across the full sky (e.g., Stern et al. 2012; Assef et al. 2013), as well as very rare populations of extremely luminous, heavily obscured AGN.

In terms of the latter, the *WISE* extragalactic team has been pursuing sources that are faint or undetected in *WISE* *W1* ($3.4 \mu\text{m}$) and *W2* ($4.6 \mu\text{m}$), but are bright in *W3* ($12 \mu\text{m}$) and *W4* ($22 \mu\text{m}$). We refer to this population as *W1W2*-dropouts (Eisenhardt et al. 2012). This is a very rare population; selecting to a depth of 1 mJy at $12 \mu\text{m}$, there are only ~ 1000 such sources across the extragalactic sky (~ 1 per 30 deg^2). These objects are undetected by *ROSAT* and tend to be optically faint ($r \gtrsim 23$), below the detection threshold of SDSS. We have obtained spectroscopic redshifts for > 100 *W1W2*-dropouts thus far, consistently finding redshifts $z \gtrsim 2$, with our current highest redshift source at $z = 4.6$ (Eisenhardt et al. 2014). Approximately half of the sources show clear type-2 AGN signatures in the optical spectra, with the other half typically showing only $\text{Ly}\alpha$ emission, sometimes extended, which could be due to star formation and/or AGN activity (Bridge et al. 2013). The lack of a far-IR peak in their broad-band SEDs suggests the dominant energy input for this population comes from a heavily obscured AGN and not extreme starbursts (e.g., Eisenhardt et al. 2012; Wu et al. 2012). Related high-luminosity sources selected from the *WISE* satellite have also recently been reported by Weedman et al. (2012) and Alexandroff et al. (2013), while several teams have identified less rare, less luminous sources from *Spitzer* surveys with less extreme colors (e.g., Dey et al. 2008; Fiore et al. 2009).

Here we report on the first targeted X-ray follow-up of *W1W2*-dropouts. We observed two sources with both the *Nuclear Spectroscopic Telescope Array* (*NuSTAR*; Harrison et al. 2013) and *XMM-Newton* (Jansen et al. 2001); a third source was only observed by *XMM-Newton*. Unless otherwise specified, we use Vega magnitudes throughout and adopt the concordance cosmology, $\Omega_M = 0.3$, $\Omega_\Lambda = 0.7$ and $H_0 = 70 \text{ km s}^{-1} \text{ Mpc}^{-1}$.

2. SAMPLE

Fig. 1 presents the optical spectra of the three *W1W2*-dropouts targeted for X-ray follow-up: WISEA J181417.29+341224.8 (hereafter, WISE J1814+3412), WISEA J220743.82+193940.1 (hereafter, WISE J2207+1939) and WISEA J235710.82+032802.8 (hereafter, WISE J2357+0328). The spectra were all obtained with the Low Resolution Imaging Spectrometer (LRIS; Oke et al. 1995) on the Keck I telescope, between 2010 July and 2010 November. The sources were selected on the basis of having unusually red colors across the *WISE* passbands in the initial All-Sky *WISE* data release: $W1 > 17.4$, $W4 < 7.7$, and $W2 - W4 > 8.2$ (for further details on the *W1W2*-dropout selection, see Eisenhardt et al. 2012). The most likely interpretation of sources with these extreme colors is that they host an extremely luminous, heavily obscured AGN which only becomes evident at observed wavelengths

$\gtrsim 10 \mu\text{m}$. The *W1* flux limit essentially constrains the sample to $z \gtrsim 1.5$ for the host galaxy not to be detected.

Note the diversity of the optical spectra of the three sources targeted for X-ray follow-up (Fig. 1). This is representative of the diverse optical spectroscopic properties of the *W1W2*-dropout population in general (Wu et al. 2012; Eisenhardt et al. 2014). Eisenhardt et al. (2012) discusses WISE J1814+3412 in depth: briefly, the optical spectrum is indistinguishable from an L^* Lyman-break galaxy (LBG) at $z \sim 2.5$ (e.g., Shapley et al. 2003), with no obvious signature of a (buried) AGN. However, typical LBGs have $22 \mu\text{m}$ flux densities a factor of 1000 lower (Reddy et al. 2006). The redshift of WISE J2207+1939 is based on a single, asymmetric, high equivalent width emission line which is reliably identified as $\text{Ly}\alpha \lambda 1216$ (for a detailed discussion of one-line redshifts, see Stern et al. 2000). WISE J2357+0328 shows a high equivalent width ($\sim 300 \text{ \AA}$, observed), slightly broadened (FWHM $\sim 1500 \text{ km s}^{-1}$), self-absorbed line identified as C IV $\lambda 1549$, which is a common strong line in AGN. However, quite unusually, no $\text{Ly}\alpha$ emission is evident. The only strong feature blue-ward of the emission line is a continuum break at observed $\sim 3785 \text{ \AA}$, which is consistent with the $\text{Ly}\alpha$ forest break for the longer wavelength emission line being C IV. Hall et al. (2004) reports on a detailed investigation of a similar SDSS quasar with broad C IV emission, but lacking broad $\text{Ly}\alpha$ emission. They argue that the unusual spectrum cannot be solely due to dust extinction in the broad line region (BLR), and instead suggest that most, but not all, of the spectral properties can be explained by an unusually high density gas in the BLR ($n_H \sim 10^{15} \text{ cm}^{-3}$) with an incident power-law continuum extending to $\geq 200 \mu\text{m}$. Clearly the unusual optical spectrum of WISE J2357+0328 is worthy of future study, but such analysis is beyond the scope of the current paper which focuses on the X-ray properties of the *W1W2*-dropout population.

In terms of their radio properties, WISE J1814+3412 has a counterpart offset by $6''.1$ in the NRAO/VLA Sky Survey (NVSS; Condon et al. 1998) with a flux density $S_{1.4 \text{ GHz}} = 3.4 \pm 0.5 \text{ mJy}$. Eisenhardt et al. (2012) report on follow-up radio observations of this source with the Jansky Very Large Array which resolves the NVSS emission into two distinct sources, the fainter of which is associated with WISE J1814+3412. Based on both its rest-frame 1.4 GHz radio luminosity ($L_{1.4 \text{ GHz}} \sim 5 \times 10^{25} \text{ W Hz}^{-1}$) and its radio-to-optical ratio (rest-frame $L_{5 \text{ GHz}}/L_{0.44 \mu\text{m}} \sim 200$), WISE J1814+3412 qualifies as radio-loud. WISE J2207+1939 has a counterpart offset by $7''.1$ in the NVSS with $S_{1.4 \text{ GHz}} = 5.2 \pm 0.4 \text{ mJy}$, suggesting that it is also radio loud. WISE J2357+0328 has no radio counterpart in either NVSS or the VLA Faint Images of the Radio Sky at Twenty Centimeters survey (FIRST; Becker et al. 1995). The radio luminosities of the first two sources further indicate the presence of a powerful AGN in this *WISE*-selected population.

3. OBSERVATIONS AND MULTIWAVELENGTH DATA

3.1. *NuSTAR* Observations

In 2012 October *NuSTAR* obtained ~ 20 ks observations of WISE J1814+3412 and WISE J2207+1939; details of the observations, including net exposure times, are provided in Table 1. We processed the level 1 data using the *NuSTAR* Data Analysis Software (*NuSTARDAS*) v.1.2.0, and produced calibrated and cleaned event files (level 2 data) for

Table 1
X-ray Observation Log.

| Target Name | z | <i>NuSTAR</i> | | | <i>XMM-Newton</i> | | |
|-----------------|-------|----------------|-------------|---------------|-------------------|-------------|----------------------------|
| | | Observation ID | UT Date | Exposure (ks) | Observation ID | UT Date | MOS1/MOS2/pn Exposure (ks) |
| (1) | (2) | (3) | (4) | (5) | (6) | (7) | (8) |
| WISE J1814+3412 | 2.452 | 60001114002 | 2012 Oct 30 | 21.3 | 0693750101 | 2012 Oct 07 | 29.6 / 29.6 / 19.6 |
| WISE J2207+1939 | 2.021 | 60001115002 | 2012 Oct 30 | 20.8 | 0693750201 | 2012 Nov 22 | 18.4 / 18.7 / 11.5 |
| WISE J2357+0328 | 2.113 | ... | ... | ... | 0693750401 | 2013 Jan 02 | 29.1 / 28.7 / 14.4 |

Note. — (1): Target name; full name and coordinates are in Table 2. (2): Redshift. (3) and (4): *NuSTAR* observation ID and start date. (5): Net on-axis *NuSTAR* exposure time. This value applies for both FPMA and FPMB. The target was on-axis for both of the *NuSTAR* observations. (6) and (7): *XMM-Newton* observation ID and start date. (8): Net on-axis exposure time, corrected for flaring and bad events, for the MOS cameras and the pn camera, as indicated.

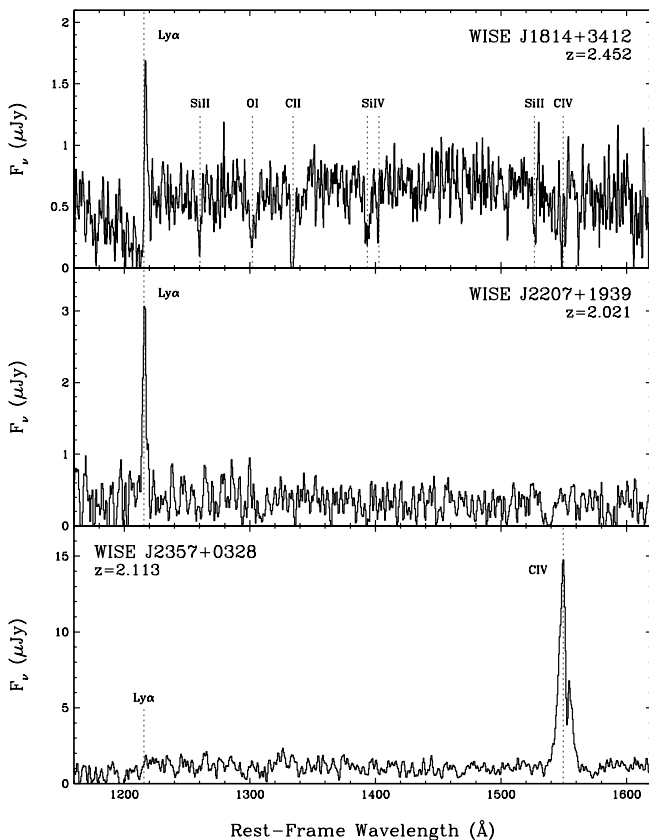


Figure 1. Keck/LRIS spectra of the three extreme *WISE*-selected obscured AGN at $z \sim 2$ which we observed at X-ray energies.

both *NuSTAR* focal plane modules (FPMA and FPMB) using *nupipeline* and the most current available version of the Calibration Database files (CALDB 20130509).

Neither source was detected, though a serendipitous broad-lined AGN at $z = 0.763$ was identified in the WISE J1814+3412 field (Alexander et al. 2013). We measured gross source counts in $45''$ radius apertures centered on the *WISE* positions and local background counts from an annulus of inner radius $90''$ and outer radius $150''$ centered on the sources. We performed photometry in the observed-frame 3–24 keV, 3–8 keV and 8–24 keV bands, as well as the rest-frame 10–40 keV band for both FPMs and used binomial statistics to determine the likelihood of the sources being detected. Binomial statistics are more accurate than Poisson statistics at these faint limits since it takes into account uncer-

tainty in the measured background (i.e., it takes the total background counts into account, not just the scaled background counts). We use binomial statistics to calculate the probability that the measured source counts are purely due to background fluctuations (i.e., false, or ‘no-source’ probabilities; for details, see Lansbury et al. 2014). For both *WISE* sources the probability of a false *NuSTAR* detection based on the binomial statistics is $> 15\%$. As we take a no-source probability $< 1\%$ to indicate a detection, neither source was detected. Since binomial statistics are not amenable to plotting simple tracks, Fig. 2 shows the X-ray counts with Poisson no-source probabilities. The latter provide a good approximation of binomial probabilities for our sources given the reasonably high background count rates.

Table 2 reports the 90% confidence limit upper limits to the flux in the 3–24 keV energy band, calculated using the Bayesian method of Kraft et al. (1991). To convert count rate to source flux, we used XSPEC v12.8.0k, taking into account the Response Matrix File (RMF) and Ancillary Response File (ARF) for each FPM. We assumed a power-law model with $\Gamma = 1.8$. Assuming a harder intrinsic spectrum does not qualitatively change these results; e.g., adopting $\Gamma = 1.0$ only changes the rest-frame 10–40 keV luminosities by $\leq 3\%$.

3.2. *XMM-Newton* Observations

We obtained ~ 30 ks observations of the three *W1W2*-dropouts between 2012 October and 2013 January with the *XMM-Newton* EPIC-MOS (Turner et al. 2001) and EPIC-pn (Strüder et al. 2001) cameras. Details of the observations are provided in Table 1. We used data products from the Pipeline Processing System (PPS), analyzed with the *Science Analysis Software*²² (SAS v.12.0.1). We measured 0.5–10 keV source counts in $15''$ radius apertures centered on the *WISE* positions. For most observations, we measured local backgrounds in slightly offset source-free circular apertures with radii of $\sim 70 - 100''$ selected to avoid serendipitous sources and chip gaps. The exceptions were the EPIC-MOS observations of WISE J2357+0328 which had no nearby serendipitous sources and thus allowed for a $30''$ to $70''$ radius annulus centered the source position. As above with the *NuSTAR* observations, we calculated binomial false probabilities and plot the equivalent using Poisson statistics in Fig. 2. Only WISE J1814+3412 is reliably detected, with a binomial no-source probability of 0.04% with EPIC-pn and 0.1% with EPIC-MOS1; WISE J1814+3412 was not reliably detected with EPIC-MOS2. WISE J2357+0328 is weakly detected

²² <http://xmm.esa.int/sas/>

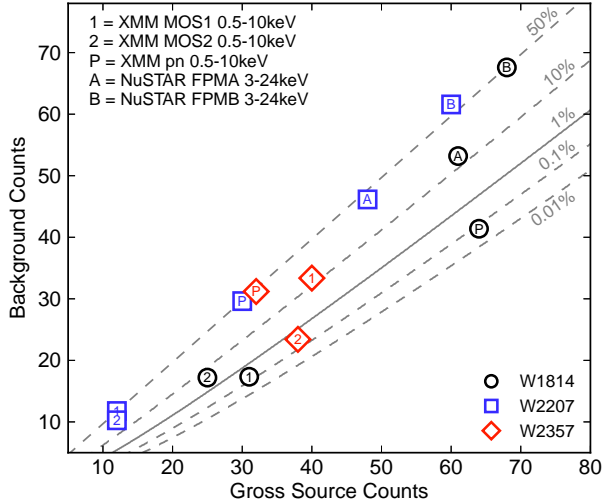


Figure 2. Gross source counts versus background counts (scaled to the source region) for WISE J1814+3412, WISE J2207+1939 and WISE J2357+0328 (circles, squares and diamonds, respectively). The 1, 2 and p labels correspond to the 0.5-10 keV counts for the EPIC-MOS1, EPIC-MOS2 and EPIC-pn cameras on *XMM-Newton*, respectively. The A and B labels correspond to the 3-24 keV counts for FPMA and FPMB on *NuSTAR*, respectively. The dashed lines indicate Poisson no-source probabilities. Two sources are faintly detected: WISE J1814+3412 is detected with the EPIC-MOS1 and EPIC-pn cameras, and WISE J2357+0328 is detected with the EPIC-MOS2 camera.

with EPIC-MOS2 with a no-source probability of 0.2%, and is undetected with the other two cameras. We used XSPEC to convert count rate (or count rate limits) to flux, assuming a power-law model with $\Gamma = 1.8$, and the *XMM-Newton* RMFs and ARFs for each EPIC camera. Again, adopting a harder intrinsic X-ray spectrum would have a modest quantitative effect on the derived luminosities, but would not affect our broad conclusions. Specifically, were we to instead assume $\Gamma = 1.0$, the rest-frame 2-10 keV luminosities would change by $\leq 18\%$.

3.3. Mid-IR Data

Table 2 presents basic source properties and multi-wavelength photometry for the three X-ray-targeted *W1W2*-dropouts. We list mid-IR data from the AllWISE data release²³ and *Spitzer*, where the latter comes from the *Warm Spitzer* observations reported by Griffith et al. (2012). Comparing the AGN luminosity and reddening of WISE J1814+3412 derived solely from the mid-IR photometry (§4.1) to the values in Eisenhardt et al. (2012) derived from 16-band multi-wavelength photometry, we obtain consistent values within $\sim 10\%$.

4. RESULTS

4.1. AGN Properties from Mid-IR Data

We modelled the spectral energy distribution (SED) of each source using the Assef et al. (2010) 0.03-30 μm empirical AGN and galaxy templates. Each SED is modelled as a best-fit, non-negative combination of an elliptical, spiral, and irregular galaxy component, plus an AGN component. Only the AGN component is fit for dust reddening (for further details on the SED models, see Assef et al. 2008, 2010).

The modeling outputs $L_{6\mu\text{m}}$, the derived intrinsic luminosity (νL_ν) of the AGN component at rest-frame $6\mu\text{m}$, as well as the reddening of the AGN component, $E(B - V)_{\text{AGN}}$ (see Table 2). For the typical gas to dust ratio observed by Maiolino et al. (2001) for luminous AGN, the nuclear reddening values of $E(B - V)_{\text{AGN}} \sim 5 - 20$ imply gas columns of $N_{\text{H}} \sim (5 - 20) \times 10^{23} \text{ cm}^{-2}$, which reach into the Compton-thick regime ($N_{\text{H}} \geq 1.5 \times 10^{24} \text{ cm}^{-2}$).

4.2. Indirect X-Ray Absorption Constraints

The mid-IR properties of *W1W2*-dropouts indicate the presence of extremely luminous, heavily obscured AGN, with bolometric luminosities approaching, or even exceeding $L_{\text{bol}} \sim 10^{14} L_{\odot}$ (Eisenhardt et al. 2012; Wu et al. 2012; Bridge et al. 2013; Assef et al. 2014; Jones et al. 2014; Tsai et al. 2014). Given the heavy obscuration implied by their mid-IR SEDs and optical spectra, it is perhaps unsurprising that the three sources we targeted for X-ray follow-up are either undetected or only faintly detected, despite observing at the penetrating energies above rest-frame 10 keV which are less affected by absorption. But what are their absorption column densities? We can obtain indirect estimates of this from their mid-IR luminosities since unobscured AGN tend to have a fairly tight relation between their mid-IR and X-ray luminosities.

Fig. 3 compares the rest-frame $6\mu\text{m}$ and X-ray luminosities for our targeted sources. We show local relations from Lutz et al. (2004), Gandhi et al. (2009) and Fiore et al. (2009), as well as non-beamed AGN with $L_X > 10^{43} \text{ erg s}^{-1}$ from the *NuSTAR* serendipitous survey (Alexander et al. 2013); the serendipitous sources all lie within the scatter of the published relations. We also show Compton-thick quasars observed at soft energies from Alexander et al. (2008), three SDSS type-2 quasars observed by *NuSTAR* (Lansbury et al. 2014), and an obscured quasar at $z \approx 2$ detected by *NuSTAR* in the Extended *Chandra* Deep Field South (ECDFS; Del Moro et al. 2014). The literature obscured AGN and the *WISE*-selected *W1W2*-dropouts generally lie significantly below the published relations. Assuming the suppression of their X-ray emission is due to absorption rather than intrinsic X-ray weakness, we can estimate their column densities from the dashed lines in Fig. 3, which apply columns of $N_{\text{H}} = 10^{24} \text{ cm}^{-2}$ to the published relations. These were calculated using the MYTorus model (Murphy & Yaqoob 2009) with photon index $\Gamma = 1.8$ and a torus inclination angle $\theta_{\text{obs}} = 70^\circ$. The implication is that all three targeted sources are obscured, possibly heavily obscured or Compton-thick. For the rest-frame 2-10 keV panel, the one detected source, WISE J1814+3412, has a column of $N_{\text{H}} \sim 10^{24} \text{ cm}^{-2}$ for the Fiore et al. (2009) relation, and yet higher columns for the other two relations. The undetected sources require minimum columns of $N_{\text{H}} \sim 10^{24} \text{ cm}^{-2}$ for all but the Fiore et al. (2009) relation. Constraints from the *NuSTAR* nondetections are less strict, but are again consistent with heavy absorption columns. Furthermore, two of the three *WISE*-selected targets are radio-loud. Since optically selected radio-loud quasars tend to have extra X-ray emission quasars as compared to radio-quiet quasars (Miller et al. 2011), this suggests yet larger minimum absorption columns for WISE J1814+3412 and WISE J2207+1939. In addition, the jet-linked X-ray emission is apparently subject to similarly high obscuration as the nuclear X-ray emission.

²³ <http://wise2.ipac.caltech.edu/docs/release/allwise/>

Table 2
Source Properties.

| | WISE J1814+3412 | WISE J2207+1939 | WISE J2357+0328 |
|----------------------------|--------------------|--------------------|--------------------|
| R.A. (J2000) | 18:14:17.29 | 22:07:43.82 | 23:57:10.82 |
| Dec. (J2000) | +34:12:24.8 | +19:39:40.1 | +03:28:02.8 |
| z | 2.452 | 2.021 | 2.113 |
| $W1$ ($3.4 \mu\text{m}$) | 18.861 ± 0.440 | 17.174 ± 0.127 | > 18.142 |
| $W2$ ($4.6 \mu\text{m}$) | 17.609 ± 0.492 | 16.136 ± 0.170 | > 16.614 |
| $W3$ ($12 \mu\text{m}$) | 10.410 ± 0.061 | 10.630 ± 0.106 | 10.088 ± 0.068 |
| $W4$ ($22 \mu\text{m}$) | 6.863 ± 0.071 | 7.135 ± 0.101 | 6.942 ± 0.112 |
| [3.6] | 17.707 ± 0.023 | 17.023 ± 0.048 | 17.487 ± 0.076 |
| [4.5] | 17.021 ± 0.020 | 16.208 ± 0.025 | 16.544 ± 0.036 |
| $f_{0.5-2 \text{ keV}}$ | 0.109 ± 0.053 | < 0.264 | < 0.243 |
| $f_{2-10 \text{ keV}}$ | < 1.30 | < 0.780 | 1.05 ± 0.53 |
| $f_{0.5-10 \text{ keV}}$ | 0.521 ± 0.141 | < 0.523 | 0.73 ± 0.31 |
| $f_{3-24 \text{ keV}}$ | < 7.55 | < 6.04 | ... |
| $L_{6\mu\text{m}}$ | 20.10 ± 2.40 | 8.28 ± 1.62 | 5.04 ± 0.36 |
| $E(B-V)_{\text{AGN}}$ | 15.1 ± 1.1 | 17.6 ± 2.3 | 5.5 ± 0.4 |
| $L_{2-10 \text{ keV}}$ | 1.04 | < 1.13 | < 1.14 |
| $L_{10-40 \text{ keV}}$ | < 17.1 | < 10.1 | ... |

Note. — Astrometry and *WISE* photometry are from the AllWISE release; mid-IR photometry is all in Vega magnitudes and *WISE* limits report the 95% confidence lower limit to the apparent magnitude. *Spitzer* photometry, in brackets, is from Griffith et al. (2012). X-ray fluxes, all in the observed frame, are in units of $10^{-14} \text{ erg cm}^{-2} \text{ s}^{-1}$. $L_{6\mu\text{m}}$ is the rest-frame $6\mu\text{m}$ luminosity (νL_ν) of the AGN in units of $10^{46} \text{ erg s}^{-1}$. Rest-frame X-ray luminosities are in units of $10^{44} \text{ erg s}^{-1}$. We report 68% confidence limit (CL) uncertainties on the X-ray fluxes; upper limits correspond to the 90% CL.

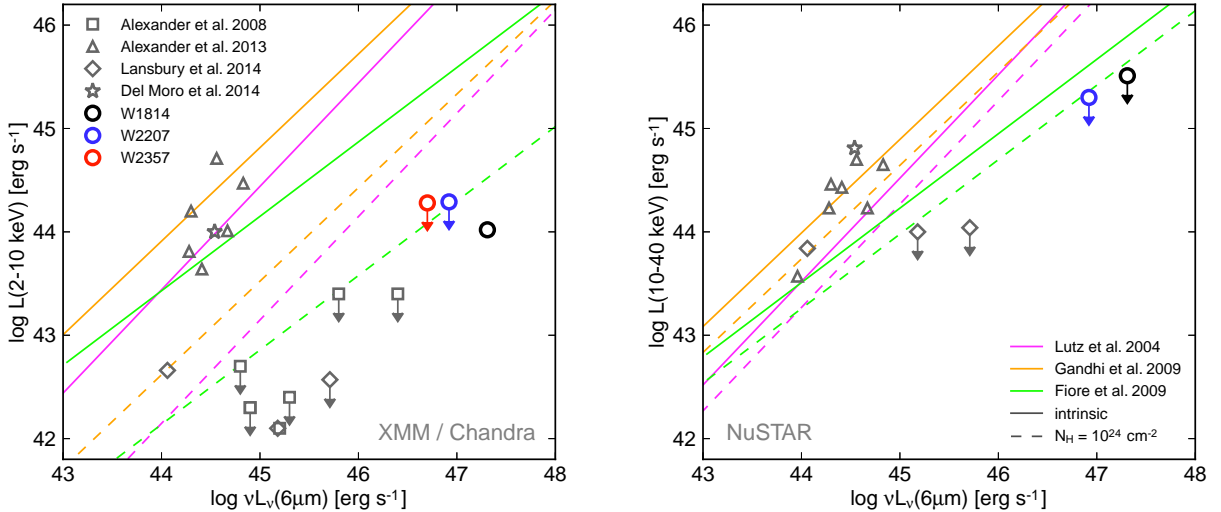


Figure 3. Rest-frame X-ray luminosity against rest-frame $6\mu\text{m}$ luminosity for: (left) 2-10 keV luminosities calculated using *XMM-Newton* data; and (right) 10-40 keV luminosities calculated using *NuSTAR* data. The X-ray luminosities are not corrected for absorption, and upper limits correspond to 3σ values to aid literature comparisons. WISE J1814+3412, WISE J2207+1939 and WISE J2357+0328 are shown as black, blue and red circles, as indicated. We compare with *NuSTAR* observations from the serendipitous survey (Alexander et al. 2013; triangles), a survey of three SDSS type-2 quasars at $z \sim 0.5$ (Lansbury et al. 2014; diamonds), and an interesting source at $z \approx 2$ detected by *NuSTAR* in the ECDFS (Del Moro et al. 2014; star); in the left panel we also show soft X-ray data on Compton-thick quasars from Alexander et al. (2008; squares). We compare with three published intrinsic relations for 2-10 keV calibrated using local AGN, as indicated. The relations are extrapolated to the 10-40 keV band assuming $\Gamma = 1.8$ and in both panels the dashed lines show the result of obscuration by $N_{\text{H}} = 10^{24} \text{ cm}^{-2}$. Assuming the low X-ray luminosities are due to absorption, sources that lie below the $N_{\text{H}} = 10^{24} \text{ cm}^{-2}$ tracks may be Compton-thick.

We designed our X-ray integration times to provide robust detections for (i) typical intrinsic AGN SEDs, and (ii) gas column densities $N_{\text{H}} \lesssim 10^{24} \text{ cm}^{-2}$. None of the three sources was strongly detected, implying that at least one of the assumptions in our experimental design does not hold.

NuSTAR has now observed a range of obscured AGN, from famous, local sources such as Mrk 231 (Teng et al. 2014), Circinus (Arévalo et al. 2014), NGC 424 (Baloković et al. 2014), and NGC 4945 (Puccetti et al. 2014), to higher red-

shift obscured quasars at $z \sim 0.5$ from SDSS (Lansbury et al. 2014) and $z \sim 2$ in the ECDFS (Del Moro et al. 2014). A recurring theme of these observations is that several AGN which are extremely luminous at certain wavelengths, such as in the mid-IR or [O III] $\lambda 5007$, remain faint at X-ray energies. For some objects, this is the case even for the more penetrating hard X-rays $> 10 \text{ keV}$. For some sources, such as optically bright ($B \lesssim 16$) broad-absorption line (BAL) quasars from the Palomar-Green (PG) survey (Schmidt & Green 1983) and

Mrk 231, we consider, and sometimes even favor attributing the hard X-ray faintness to intrinsic X-ray weakness (Luo et al. 2013; Teng et al. 2014). Such intrinsic X-ray weakness seems the most plausible scenario when the AGN appears unobscured at certain wavelengths, through strong UV continuum emission, broad emission lines, and/or weak X-ray spectra that are well described by a moderately absorbed power-law. For a more detailed description of the intrinsically X-ray weak scenario, see Luo et al. (2013) and Teng et al. (2014).

For the three *WISE*-selected AGN discussed here, we instead favor interpreting the X-ray faintness as being due to a typical AGN seen through extremely high absorbing columns, consistent with their mid-IR SEDs and optical spectra. Indeed, the X-ray column constraints from Fig. 3 are broadly consistent with the mid-IR measurements given typical luminous AGN gas-to-dust ratios from Maiolino et al. (2001). What is more surprising is that these sources, amongst the bolometrically most luminous AGN known, appear heavily obscured. Various observations have shown that more luminous AGN are less likely to be obscured (e.g., Ueda et al. 2003; Simpson 2005; Assef et al. 2013). This is consistent with the “receding torus model”, first proposed by Lawrence (1991), in which the height of the torus is independent of luminosity while the inner radius of the torus, corresponding to the distance at which dust reaches its sublimation temperature, increases with luminosity. Therefore, in this model, more luminous AGN have more sightlines into the nucleus and thus have a lower likelihood of being obscured.

The *W1W2*-dropout population is a rare population, with a surface density of just one source per $\sim 30 \text{ deg}^2$ in the extragalactic sky. The mid-IR luminosities imply intrinsic X-ray luminosities of a few $\times 10^{45} \text{ erg s}^{-1}$ from the relations of Lutz et al. (2004) and Gandhi et al. (2009). Just et al. (2007) report on X-ray follow-up of the most luminous quasars in the SDSS available at the time, finding 34 quasars across 4188 deg^2 , or one source per $\sim 120 \text{ deg}^2$. The X-ray luminosities of this luminous quasar sample prove comparable to the expected intrinsic X-ray luminosities from the *WISE*-selected sample, implying the surprising discovery of comparable numbers of obscured and unobscured quasars at the top of the luminosity function. Assef et al. (2014) and Tsai et al. (2014) present more detailed comparisons between the *W1W2*-dropout and luminous unobscured quasar populations.

The discovery of a significant population of heavily obscured, extremely luminous AGN does not conform to the simple receding torus model, suggesting an additional source of obscuration. Indeed, the models of Draper & Ballantyne (2010) predict that Compton-thick AGN should be more common at higher redshift because of the high fueling rates of quasars require significant gas reservoirs. This is consistent with models showing that mergers may be more prominent in fueling AGNs at $z \sim 2$ (e.g., Hopkins et al. 2008; Draper & Ballantyne 2012). Indeed, these models also predict that the unified model of AGN will break down for high-luminosity AGNs at $z \gtrsim 1$ because the obscuration is not confined to the nucleus (see also Draper & Ballantyne 2011).

Further investigations into this interesting population are clearly warranted. Deeper X-ray observations, achieving robust detections rather than faint and non-detections, would be valuable. For example, assuming the obscuration is from a nuclear torus, deeper X-ray observations should detect narrow,

reflected Fe $K\alpha$ fluorescent emission at rest-frame 6.4 keV (e.g., Nandra et al. 2007); a significant non-detection could point towards obscuration on larger scales than the torus. Such large-scale obscuration could also be probed by high-resolution imaging, such as far-IR observations with ALMA, and, eventually, mid-IR observations with *JWST*. Near-IR spectroscopy could also look for reddening in the AGN narrow-line region (e.g., Brand et al. 2007), which is expected to be significantly larger than the torus. A clearer understanding of the geometry of the obscuring region combined with an improved reckoning of the *W1W2*-dropout space density will enable us to better place this population within the context of AGNs and galaxy evolution.

This work was supported under NASA Contract No. NNG08FD60C, and made use of data from the *NuSTAR* mission, a project led by the California Institute of Technology, managed by the Jet Propulsion Laboratory, and funded by the National Aeronautics and Space Administration. We thank the *NuSTAR* Operations, Software and Calibration teams for support with the execution and analysis of these observations. This research has made use of the *NuSTAR* Data Analysis Software (NuSTARDAS) jointly developed by the ASI Science Data Center (ASDC, Italy) and the California Institute of Technology (USA). This publication makes use of data products from the *Wide-field Infrared Survey Explorer*, which is a joint project of the University of California, Los Angeles, and the Jet Propulsion Laboratory/California Institute of Technology, funded by the National Aeronautics and Space Administration. We acknowledge financial support from the Science and Technology Facilities Council (STFC) grants ST/K501979/1 (GBL), ST/I001573/1 (DMA and ADM) and ST/J003697/1 (PG). RJA was supported by Gemini-CONICYT grant number 32120009. RCH acknowledges support from NASA through ADAP award NNX12AE38G and the National Science Foundation through grant number 1211096.

Facilities: Keck (LRIS), NuSTAR, Spitzer (IRAC), XMM-Newton, WISE

©2014. All rights reserved.

REFERENCES

- Alexander, D. M., Chary, R.-R., Pope, A., et al. 2008, *ApJ*, 687, 835
 Alexander, D. M., Stern, D., Del Moro, A., et al. 2013, *ApJ*, 773, 125
 Alexandroff, R., Strauss, M. A., Greene, J. E., et al. 2013, *MNRAS*, 435, 3306
 Arévalo, P., Bauer, F., et al. 2014, *ApJ*, submitted
 Assef, R. J., Kochanek, C. S., Brodwin, M., et al. 2008, *ApJ*, 676, 286
 —. 2010, *ApJ*, 713, 970
 Assef, R. J., Stern, D., Kochanek, C. S., et al. 2013, *ApJ*, 772, 26
 Assef, R. J. et al. 2014, *ApJ*, in prep.
 Baloković, M., Comastri, A., Harrison, F. A., et al. 2014, *ApJ*, submitted
 Becker, R. H., White, R. L., & Helfand, D. J. 1995, *ApJ*, 450, 559
 Brand, K., Dey, A., Desai, V., et al. 2007, *ApJ*, 663, 204
 Bridge, C., Blain, A., Borys, C., et al. 2013, *ApJ*, 769, 91
 Condon, J. J., Cotton, W. D., Greisen, E. W., et al. 1998, *AJ*, 115, 1693
 Del Moro, A., Mullaney, J. R., Alexander, D. M., et al. 2014, *ApJ*, submitted
 Dey, A. et al. 2008, *ApJ*, 677, 943
 Donley, J. L., Koekemoer, A. M., Brusa, M., et al. 2012, *ApJ*, 748, 142
 Draper, A. R. & Ballantyne, D. R. 2010, *ApJ*, 715, 99
 —. 2011, *ApJ*, 729, 109
 —. 2012, *ApJ*, 753, 37
 Eisenhardt, P. R., Wu, J., Tsai, C., et al. 2012, *ApJ*, 755, 173
 Eisenhardt, P. R. et al. 2014, *ApJ*, in prep.
 Fiore, F., Puccetti, S., Brusa, M., et al. 2009, *ApJ*, 693, 447
 Gandhi, P., Horst, H., Smette, A., et al. 2009, *A&A*, 502, 457

- Griffith, R. L., Kirkpatrick, J. D., Eisenhardt, P., et al. 2012, *AJ*, 144, 148
- Hall, P. B., Snedden, S. A., Niederste-Ostholt, M., Eisenstein, D. J., Strauss, M. A., York, D. G., & Schneider, D. P. 2004, *AJ*, 128, 534
- Harrison, F. A., Craig, W. W., Christensen, F. E., et al. 2013, *ApJ*, 770, 103
- Hopkins, P. et al. 2008, *ApJS*, 175, 356
- Jansen, F., Lumb, D., Altieri, B., et al. 2001, *A&A*, 365, 1
- Jones, S. F., Blain, A. W., Stern, D., et al. 2014, *MNRAS*, submitted
- Just, D., Brandt, W. N., Shemmer, O., Steffen, A. T., Schneider, D. P., Chartas, G., & Garmire, G. 2007, *ApJ*, 665, 1004
- Kraft, R. P., Burrows, D. N., & Nousek, J. A. 1991, *ApJ*, 374, 344
- Lansbury, G. B., Alexander, D. M., Del Moro, A., et al. 2014, *ApJ*, in press (arXiv:1402.2666)
- Lawrence, A. 1991, *MNRAS*, 252, 586
- Luo, B., Brandt, W. N., Alexander, D. M., et al. 2013, *ApJ*, 772, 125
- Lutz, D., Maiolino, R., Spoon, H. W. W., & Moorwood, A. F. M. 2004, *A&A*, 418, 465
- Maiolino, R., Marconi, A., Salvati, M., Risaliti, G., Severgnini, P., Oliva, E., La Franca, F., & Vanzi, L. 2001, *A&A*, 365, 28
- Miller, B. P., Brandt, W. N., Schneider, D. P., Gibson, R. R., Steffen, A. T., & Wu, J. 2011, *ApJ*, 726, 20
- Murphy, K. D. & Yaqoob, T. 2009, *MNRAS*, 397, 1549
- Nandra, K., O'Neill, P. M., George, I. M., & Reeves, J. N. 2007, *MNRAS*, 382, 194
- Oke, J. B., Cohen, J. G., Carr, M., et al. 1995, *PASP*, 107, 375
- Puccetti, S. et al. 2014, *ApJ*, in prep.
- Reddy, N. A., Steidel, C. C., Fadda, D., et al. 2006, *ApJ*, 644, 792
- Schmidt, M. & Green, R. F. 1983, *ApJ*, 269, 352
- Shapley, A. E., Steidel, C. C., Pettini, M., & Adelberger, K. L. 2003, *ApJ*, 588, 65
- Simpson, C. 2005, *MNRAS*, 360, 565
- Stern, D., Assef, R. J., Benford, D. J., et al. 2012, *ApJ*, 753, 30
- Stern, D., Bunker, A. J., Spinrad, H., & Dey, A. 2000, *ApJ*, 537, 73
- Stern, D., Eisenhardt, P., Gorjian, V., et al. 2005, *ApJ*, 631, 163
- Strüder, L., Briel, U., Dennerl, K., et al. 2001, *A&A*, 365, L18
- Teng, S. H., Brandt, W. N., Harrison, F. A., et al. 2014, *ApJ*, in press (arXiv:1402.4811)
- Tsai, C. et al. 2014, *ApJ*, in prep.
- Turner, M. J. L., Abbey, A., Arnaud, M., et al. 2001, *A&A*, 365, L27
- Ueda, Y., Akiyama, M., Ohta, K., & Mijaji, T. 2003, *ApJ*, 598, 886
- Weedman, D., Sargsyan, L., Leboutteiller, V., Houck, J., & Barry, D. 2012, *ApJ*, 761, 184
- Wright, E. L., Eisenhardt, P. R. M., Mainzer, A. K., et al. 2010, *AJ*, 140, 1868
- Wu, J., Tsai, C., Sayers, J., et al. 2012, *ApJ*, 756, 96